JOURNAL OF COMPUTATIONAL PHYSICS 108, 306–313 (1993)

Finite-Difference Schemes on Regular Triangular Grids

DAVID W. ZINGG

Institute for Aerospace Studies, University of Toronto, Toronto, Ontario, Canada M3H 5T6

AND

HARVARD LOMAX

NASA Ames Research Center, Moffett Field, California 94035

Received September 19, 1990; revised October 11, 1991

The phase error and isotropy properties of various finite-difference schemes on grids consisting of regular triangles are compared with similar schemes on square grids. The comparisons are based on a Fourier analysis of semidiscrete solutions to the two-dimensional linear convection equation. The finite-difference schemes presented on the triangular grid include a second-order method, a compact fourth-order method, and a modified compact method designed to extend the accurate wave number range of the numerical approximation. All of the schemes considered are centered and hence nondissipative. In each case, the finite-difference scheme on the triangular grid reduces the anisotropy of the phase error in comparison with a similar scheme on the square grid.

1. INTRODUCTION

Discretization of a partial differential equation introduces phase error and thus numerical dispersion. In multidimensions, the phase error has a dependence on the direction of propagation and consequently is anisotropic. The anisotropy of numerical phase error has been studied by numerous authors, including Bamberger *et al.* [1], Lele [2], Mullen and Belytschko [3], Trefethen [4], and Vichnevetsky and Bowles [6]. Mullen and Belytschko [3] studied various semidiscretizations of the two-dimensional wave equation on quadrilateral and triangular meshes. Several different triangular mesh configurations were considered. A triangular mesh consisting of regular triangles was shown to produce the lowest anisotropy of the phase error.

The purpose of this paper is to compare the phase error resulting from several finite-difference semidiscretizations of the two-dimensional linear convection equation on square and triangular meshes. All of the semidiscretizations compared are centered and hence are nondissipative. The finite-difference schemes studied on the triangular mesh include a second-order method, a compact fourth-order method, and an extended-wave-number method. An extended-wave-number method maximizes the range of wave numbers for which the scheme achieves some specified accuracy rather than the order of accuracy of the scheme. This concept, originally suggested by Vichnevetsky and De Schutter [7], was explored in detail by Lele [2] for one-dimensional and square meshes.

Section 2 reviews some well-known concepts relating to numerical phase error in one dimension. Isotropy errors on a square mesh are reviewed in Section 3. Section 4 presents the finite-difference schemes and the associated isotropy errors on a triangular mesh. A discussion and conclusions are given in Sections 5 and 6.

2. WAVE PROPAGATION ERRORS IN ONE DIMENSION

This section is a brief review of some well-known material. It is included to clarify terminology and concepts used in the following sections.

Exact solution. Consider the one-dimensional linear convection equation given by

$$\frac{\partial U}{\partial t} + c\frac{\partial U}{\partial x} = 0, \tag{2.1}$$

where $U(x, t)$ is a scalar propagating with phase speed c. A solution initiated by a harmonic function with wave number κ is

$$U(x, t) = u(t)\, e^{i\kappa x}, \tag{2.2}$$

where $u(t)$ satisfies the ordinary differential equation

$$\frac{du}{dt} = -ic\kappa u. \tag{2.3}$$

0021-9991/93 $5.00

Solving for $u(t)$ and inserting the result in Eq. (2.2), one finds

$$U(x, t) = u(0)\, e^{i(\kappa x - \omega t)}, \tag{2.4}$$

where the frequency ω and wave number κ are related by the phase speed, c, through the relation

$$\omega = c\kappa. \tag{2.5}$$

The group velocity, the velocity at which waves transport energy, is given by

$$c_g = d\omega/d\kappa. \tag{2.6}$$

If the phase speed is a constant, independent of the wave number κ, we see from Eq. (2.6) that the group velocity is equal to the phase speed, and the system is said to be nondispersive.

Semidiscrete methods. Next consider some numerical semidiscrete approximations of Eq. (2.1). This terminology is used to describe the approach in which only the spatial derivatives are discretized, and the governing system is reduced to a set of ordinary differential equations.

Explicit Schemes

For a simple example, use the second-order-accurate three-point centered difference scheme on an equispaced mesh with spacing L. (In this case $L = \Delta x$, but later it represents the length of the side of a square or a regular triangle.)

$$(\delta_x U)_j = \frac{1}{2L}(U_{j+1} - U_{j-1}), \tag{2.7}$$

where $x_j = jL$ and $U_j = U(x_j, t) = u(t)\, e^{i\kappa(jL)}$. Using Eq. (2.7) for the space derivative in Eq. (2.1), with the initial condition imposed by Eq. (2.2), we are led to the ordinary differential equation given by

$$\frac{du}{dt} = -ic\kappa\left[\frac{\sin(\kappa L)}{\kappa L}\right]u = -ic^*\kappa u = -ic\kappa^* u. \tag{2.8}$$

The term $[\sin(\kappa L)/(\kappa L)]$ represents the error caused by the space differencing. We can regard it as an error in wave number or as an error in phase speed. We define the terms c^* as *numerical phase speed*, κ^* as *numerical* (or *modified*) *wave number*, $\omega^* = \kappa c^* = c\kappa^*$ as *numerical frequency*, and $err_{\text{phase}} = (c - c^*)/c$ as the numerical phase speed error. In our example,

$$c^* = \frac{c}{\kappa L}\sin(\kappa L) \tag{2.9}$$

and the numerical group velocity is

$$c_g^* = \frac{d\omega^*}{d\kappa} = c\cos(\kappa L). \tag{2.10}$$

The latter is the speed at which the numerical solution will propagate a wave packet [4, 5].

For later generalizations we express the numerical phase speed as

$$c^* = \frac{c}{\kappa L} f^*(\kappa L) \tag{2.11}$$

and note that the form of $f^*(\kappa L)$ depends on the choice of differencing scheme.

Padé (or Implicit or Compact or Hermite) Schemes

For a simple Padé example, consider the fourth-order-accurate three-point central difference scheme

$$(\delta_x U)_{j-1} + 4(\delta_x U)_j + (\delta_x U)_{j+1} = \frac{3}{L}(U_{j+1} - U_{j-1}). \tag{2.12}$$

Following the above development, we are led again to Eq. (2.11), where in this case

$$f^*(\kappa L) = \frac{3\sin(\kappa L)}{2 + \cos(\kappa L)}. \tag{2.13}$$

Extended Wave Number Schemes

The Fourier analysis of finite difference approximations to first and second space derivatives is a widely used technique for comparing schemes. In these comparisons we can think of κ as the input wave number and $\kappa^* = f^*/L$, see Eq. (2.11), as the output or modified wave number. This provides a way to extend our classification of methods beyond the concept of "order of accuracy," which gives information only about the low wave number resolution, to include the entire wave number range available in a mesh of given size (the maximum available accuracy from a differencing scheme is no error at all for the entire range $0 \leqslant \kappa L < \pi$, and is provided by a spectral method).

The idea of using some of the coefficients in the development of a finite difference scheme for extending its accurate wave number range is contained in Vichnevetsky and De Schutter [7] and highly developed by Lele [2], who refers to these methods as "spectral-like schemes." For example, using Lele's notation, we can approximate a first derivative by the scheme

$$\alpha(\delta_x U)_{j-1} + (\delta_x U)_j + \alpha(\delta_x U)_{j+1} = \frac{b}{4L}(U_{j+2} - U_{j-2}) + \frac{a}{2L}(U_{j+1} - U_{j-1}), \tag{2.14}$$

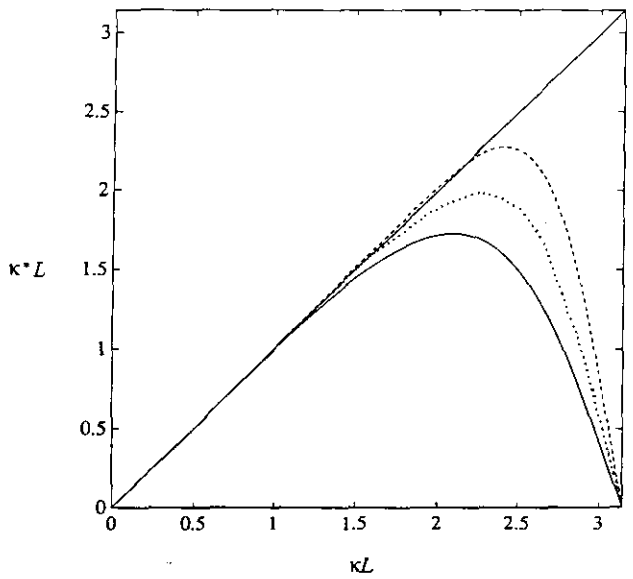

FIG. 1. Modified wave numbers from Eq. (2.14) (———, fourth-order, $\alpha = \frac{1}{4}$; ..., sixth-order, $\alpha = \frac{1}{3}$; – – –, extended scheme, $\alpha = \frac{5}{13}$).

where $a = 2(\alpha + 2)/3$ and $b = (4\alpha - 1)/3$, and we can provide a method that is fourth-order accurate for all α. With $\alpha = \frac{1}{4}$ we have the classical Padé fourth-order scheme, and with $\alpha = \frac{1}{3}$ the scheme is sixth-order accurate. A plot of the modified wave number versus the input wave number is given in Fig. 1 for $\alpha = \frac{1}{4}$, $\frac{1}{3}$, and $\frac{5}{13}$. We see that for a small allowable error in approximating a wave number, $\alpha = \frac{5}{13}$ is the best even though its formal accuracy is not the highest. In Section 4 we examine this concept further in two dimensions.

3. ISOTROPY ERRORS ON A SQUARE MESH

Fourier analysis. In two (and three) dimensions the numerical phase speed and numerical dispersion errors can vary with the angle that the propagation vector makes with the mesh. This is referred to as isotropy error. Isotropy errors are well documented for finite difference schemes developed for square meshes [1–4, 6], but we briefly review them here to contrast with the methods developed for triangular meshes that are discussed in the next section.

The partial differential equation governing a simple two-dimensional plane wave convecting the scalar quantity $U(x, y, t)$ with speed c along a straight line making an angle θ with respect to the x-axis is

$$\frac{\partial U}{\partial t} + c\cos\theta\frac{\partial U}{\partial x} + c\sin\theta\frac{\partial U}{\partial y} = 0. \tag{3.1}$$

If we choose for the initial condition a harmonic function with wave number κ,

$$U(x, y, t) = u(t)\, e^{i\kappa\xi}, \tag{3.2}$$

where

$$\xi = x\cos\theta + y\sin\theta, \tag{3.3}$$

the exact solution is

$$U(x, y, t) = u(t)\, e^{i\kappa(\xi - ct)}. \tag{3.4}$$

In Section 2 we reviewed a way to Fourier-analyze the numerical phase speed error for difference schemes in one dimension. A similar analysis applies for two dimensional schemes on square meshes which use the same one-dimensional method in both directions. It is not difficult to show that in two dimensions,

$$c^*(\kappa L, \theta) = \frac{c}{\kappa L}(\cos\theta f^*(\kappa L\cos\theta) + \sin\theta f^*(\kappa L\sin\theta)), \tag{3.5}$$

where $f^*(\kappa L)$ is the one-dimensional numerical phase speed function defined in Eq. (2.11).

In two dimensions the wave number is a vector given for a plane wave by

$$\boldsymbol{\kappa} = \hat{\imath}\kappa\cos(\theta) + \hat{\jmath}\kappa\sin(\theta), \tag{3.6}$$

where $\hat{\imath}$ and $\hat{\jmath}$ are unit vectors along the x and y directions, respectively. The group velocity is now

$$\mathbf{c}_g = \nabla_{\boldsymbol{\kappa}}\omega^*, \tag{3.7}$$

where $\nabla_{\boldsymbol{\kappa}}$ denotes the gradient with respect to $\boldsymbol{\kappa}$ [4]. Note that, although the numerical phase velocity vector is aligned in the correct direction, the numerical group velocity vector is not.

Explicit Five-Point Cross

Using the explicit three-point centered scheme to approximate both spatial derivatives in Eq. (3.1) (giving a five-point cross stencil in two dimensions), we find the numerical phase speed to be

$$c^* = \frac{c}{\kappa L}(\cos\theta[\sin(\kappa L\cos\theta)] + \sin\theta[\sin(\kappa L\sin\theta)]). \tag{3.8}$$

Figure 2 (shown also in [2, 6]) is a plot of Eq. (3.8), showing c^*/c as a function of θ for $\lambda/L = 2, 3, 4, 8$, where the wave length λ equals $2\pi/\kappa$. This figure illustrates the lack of isotropy that occurs with the use of square meshes. Clearly the preferred direction of propagation is $\theta = 45°$, while the largest error occurs along the lines at 0° and 90°. One can

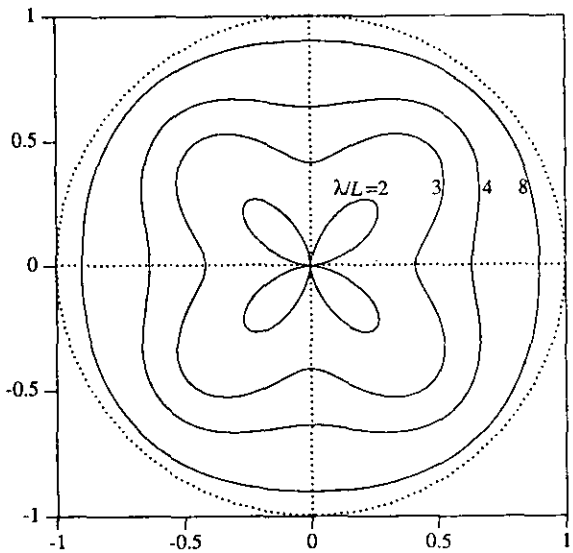

FIG. 2. Polar plot of the ratio of numerical phase speed to true phase speed for the explicit second-order five-point cross scheme on a square mesh.

show from Eq. (3.8) that the leading term in the Taylor series expansion for the phase speed error is

$$\mathrm{err}_{\mathrm{phase}} \approx \tfrac{1}{6}\kappa^2 L^2(\cos^4\theta + \sin^4\theta). \tag{3.9}$$

By this measure, even for acceptable accuracies, the error at $\theta = 0°$ and 90° is twice the error at 45°.

Explicit Nine-Point Cross

For the fourth-order explicit nine-point cross, one finds the leading term in the phase speed error expansion to be

$$\mathrm{err}_{\mathrm{phase}} \approx \tfrac{1}{30}\kappa^4 L^4(\cos^6\theta + \sin^6\theta). \tag{3.10}$$

The error at 0° and 90° is now four times the error at 45°.

Padé Five-Point Cross

For the Padé five-point cross the leading term in the error in phase speed is

$$\mathrm{err}_{\mathrm{phase}} \approx \tfrac{1}{180}(\kappa L)^4(\cos^6\theta + \sin^6\theta). \tag{3.11}$$

Although the truncation error is $\frac{1}{6}$ of that found for the explicit nine-point cross, the dependence on θ is identical.

Explicit Nine-Point Square

A second-order method can also be found using a nine-point square stencil. The resulting method, studied in Refs. [4, 6], has for the leading term in the phase speed error,

$$\mathrm{err}_{\mathrm{phase}} \approx \tfrac{1}{6}\kappa^2 L^2[(1-3\beta)(\cos^4\theta + \sin^4\theta) + 3\beta], \tag{3.12}$$

where β is a free parameter. The standard explicit five-point cross is obtained by setting $\beta = 0$. Note that when $\beta = \frac{1}{3}$, the method is, to lowest order, isotropic. Unfortunately, however, by comparing these results with those in Eq. (3.9), we see that this improved isotropy has been achieved by *increasing* the error at $\theta = 45°$ *without reducing* the error at $\theta = 0°$ or 90°. In other words, we have improved isotropy at accurate wave numbers, but we have done so by making the error in all directions equal to the *worst* error in the anisotropic case. In the next section we show that we can achieve better results with fewer points by using a mesh consisting of regular triangles, so we do not pursue this approach further.

4. ISOTROPY ERRORS ON A MESH OF REGULAR TRIANGLES

In this section we present finite-difference schemes for the two-dimensional plane wave equation (3.1) on a grid composed of regular triangles with sides of length L. The numbering system for the triangular grid is shown in Fig. 3. Three schemes are presented; all use the points numbered 0 through 6 in the figure. The first is an explicit method, the second is a Padé method, and the third is a modified Padé method designed to extend the wave number range of the numerical approximation.

Explicit, second-order method. The coefficients multiplying the dependent variables at the numbered points in Fig. 3 are found such that the approximation is second order. Even under this constraint there remains a free parameter. The value of this parameter is chosen by making the phase speed error isotropic to lowest order. The following scheme emerges:

$$\begin{aligned}(\delta_x U)_0 &= \frac{1}{3L}(U_3 - U_6) + \frac{1}{6L}(U_2 + U_4 - U_1 - U_5)\\ (\delta_y U)_0 &= \frac{\sqrt{3}}{6L}(U_1 + U_2 - U_4 - U_5).\end{aligned} \tag{4.1}$$

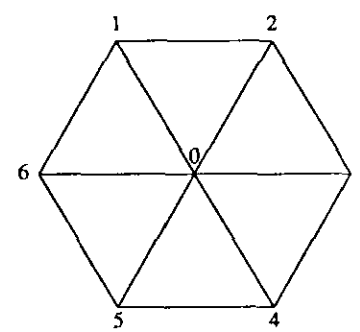

FIG. 3. Numbering system for the triangular mesh.

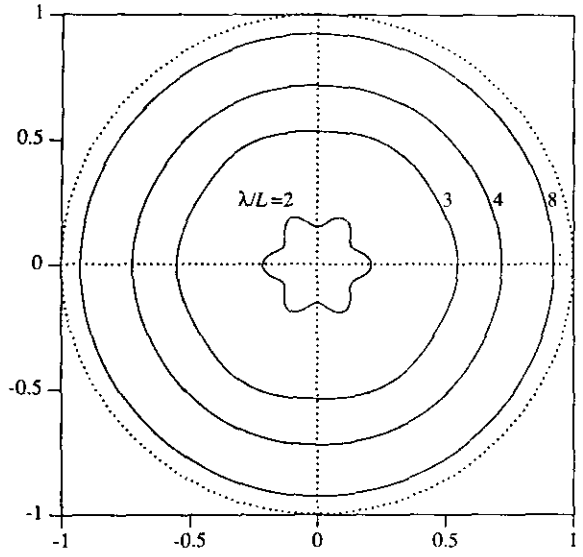

FIG. 4. Polar plot of the ratio of numerical phase speed to true phase speed for the explicit second-order scheme on the triangular mesh.

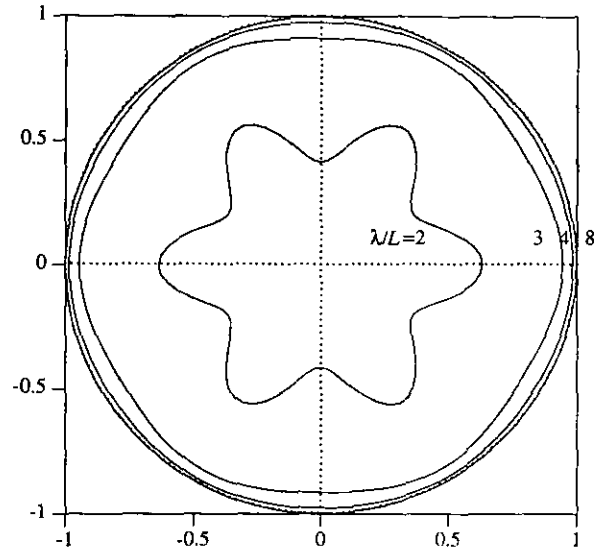

FIG. 5. Polar plot of the ratio of numerical phase speed to true phase speed for the compact fourth-order scheme on the triangular mesh.

From this

$$c^* = \frac{2}{3}\frac{c}{\kappa L}\cos\theta\left[\cos\left(\frac{\sqrt{3}\,\kappa L\sin\theta}{2}\right)\times\sin\left(\frac{\kappa L\cos\theta}{2}\right)+\sin(\kappa L\cos\theta)\right] + \frac{2}{\sqrt{3}}\frac{c}{\kappa L}\sin\theta\left[\cos\left(\frac{\kappa L\cos\theta}{2}\right)\sin\left(\frac{\sqrt{3}\,\kappa L\sin\theta}{2}\right)\right]. \tag{4.2}$$

This result for c^*/c is plotted in Fig. 4 for $\lambda/L = 2, 3, 4, 8$. When the error is very large (at $\lambda/L = 2$, for example), the preferred direction is obvious and occurs along lines separated by 60°, starting at the x-axis. The scheme is nearly isotropic for values of λ/L greater than three and the leading term in the phase speed error is

$$\text{err}_{\text{phase}} \approx (\kappa L)^2/8. \tag{4.3}$$

This should be compared with the result for the explicit nine-point square scheme with $\beta = \frac{1}{3}$ given in Eq. (3.12).

Padé fourth-order scheme. A compact fourth-order scheme using the points shown in Fig. 3 is given by

$$6(\delta_x U)_0 + \sum_{i=1}^{6}(\delta_x U)_i = \frac{4}{L}(U_3 - U_6) + \frac{2}{L}(U_2 + U_4 - U_1 - U_5) \tag{4.4}$$

$$6(\delta_y U)_0 + \sum_{i=1}^{6}(\delta_y U)_i = \frac{2\sqrt{3}}{L}(U_1 + U_2 - U_4 - U_5).$$

In this case the coefficients were chosen to make the method fourth-order accurate. Again this constraint still permitted a free parameter, and again this parameter was chosen to minimize the dependence of the error on θ. The resulting numerical phase speed is given by

$$c^* = \frac{12c_2^*}{\left(\begin{array}{c}4\cos((\kappa L\cos\theta)/2)\cos((\sqrt{3}\,\kappa L\sin\theta)/2)\\ +\,2\cos(\kappa L\cos\theta)+6\end{array}\right)}, \tag{4.5}$$

where c_2^* is the numerical phase speed of the second-order explicit scheme given by Eq. (4.2). The results for c^*/c are shown in Fig. 5. They are similar in form to those in Fig. 4, but the magnitude of the error is reduced. The leading term in the phase speed error is now

$$\text{err}_{\text{phase}} \approx \frac{(\kappa L)^4}{960}(2\cos^6\theta + 15\cos^4\theta\sin^2\theta + 3\sin^6\theta). \tag{4.6}$$

The ratio of maximum to minimum error is 1.5.

Extended wave number scheme (Padé). We now generalize the Padé scheme just presented, exploring the extended wave number concept described in Section 2. The scheme

$$(1-\beta)(\delta_x U)_0 + \frac{\beta}{6}\sum_{i=1}^{6}(\delta_x U)_i = \frac{1}{6L}[2(U_3 - U_6) + (U_2 + U_4 - U_1 - U_5)]$$

$$(1-\beta)(\delta_y U)_0 + \frac{\beta}{6}\sum_{i=1}^{6}(\delta_y U)_i = \frac{\sqrt{3}}{6}(U_1 + U_2 - U_4 - U_5) \tag{4.7}$$

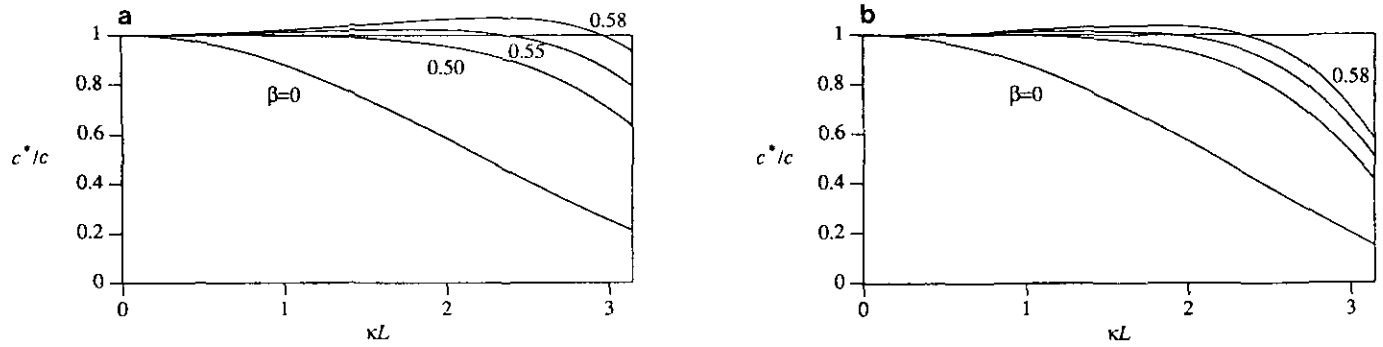

FIG. 6. Ratio of numerical phase speed to true phase speed for the extended wave number scheme on the triangular mesh with $\beta = 0, 0.50, 0.55, 0.58$; (a) $\theta = 0°$, (b) $\theta = 30°$.

is at least second-order accurate for all β. The explicit second-order scheme, Eq. (4.1), is found by setting $\beta = 0$, and the compact fourth-order scheme, Eq. (4.4), is found by setting $\beta = \frac{1}{2}$. The numerical phase speed is given by

$$c^* = \frac{c_2^*}{\left((\beta/6)[4\cos((\kappa L\cos\theta)/2)\cos((\sqrt{3}\,\kappa L\sin\theta)/2) + 2\cos(\kappa L\cos\theta)] + (1-\beta)\right)}, \tag{4.8}$$

where c_2^* is again the numerical phase speed given by Eq. (4.2). This formula is plotted for various β at $\theta = 0°$, where the method is most accurate, Fig. 6a, and at $\theta = 30°$, where the method is least accurate, Fig. 6b. Figure 7 shows a polar plot of the numerical phase speed for $\beta = 0.55$. The leading term in the truncation error is

$$\text{err}_{\text{phase}} \approx (1-2\beta)\frac{(\kappa L)^2}{8}. \tag{4.9}$$

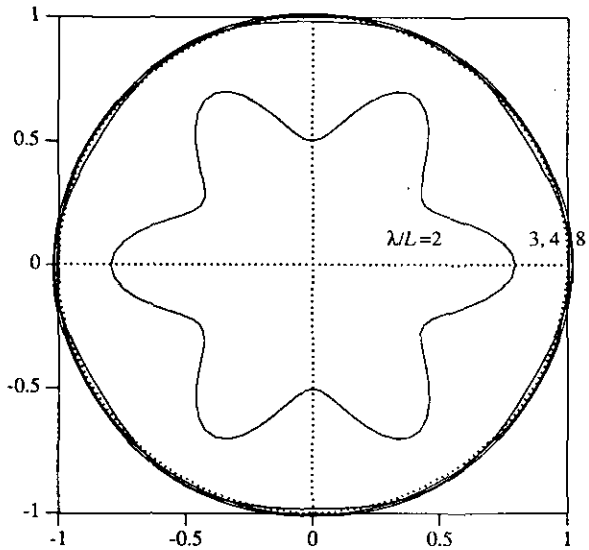

FIG. 7. Polar plot of the ratio of numerical phase speed to true phase speed for the extended wave number scheme on the triangular mesh with $\beta = 0.55$.

To second-order the method is isotropic. In this case sacrificing the fourth-order accuracy not only extended the useful wave number range, but it also improved the isotropy about the mean.

5. DISCUSSION OF RESULTS

We compare the phase error and isotropy properties of finite difference schemes constructed on square grids with those constructed on triangular grids. The comparisons are based on a Fourier analysis of semidiscrete solutions to the linear convection equation $u_t + \mathbf{c}\cdot\nabla u = 0$. All of the examples considered are based on centered schemes and no attention is paid to the effect of boundary conditions. Thus there is no mechanism to produce dissipation and the numerical errors are all related to the phase speed, wave number, and frequency. There are three measures of error that are considered:

1. The conventional order of accuracy based on a Taylor series expansion in terms of the mesh characteristic length.

2. The range of wave numbers a scheme can approximate and stay within some given error bound.

3. The dependency of the above two errors on the angle the wave makes with the mesh, that is, isotropy error.

Some of our results are summarized in Tables I and II, which compare the lowest order truncation term of the seven differencing schemes we have analyzed. Only three of

TABLE I

Summary of Results for Square Mesh

Scheme on square mesh	Phase speed error to lowest order
Explicit, 5-point cross	$\frac{1}{6}(\kappa L)^2(\cos^4\theta + \sin^4\theta)$
Explicit, 9-point cross	$\frac{1}{30}(\kappa L)^4(\cos^6\theta + \sin^6\theta)$
Explicit, 9-point square	$\frac{1}{6}(\kappa L)^2$
Padé, 5-point cross	$\frac{1}{180}(\kappa L)^4(\cos^6\theta + \sin^6\theta)$

TABLE II

Summary of Results for Mesh of Regular Triangles

Scheme on triangular mesh	Phase speed error to lowest order
Explicit, 7-point	$\frac{1}{8}(\kappa L)^2$
Padé, 7-point	$\frac{1}{960}(\kappa L)^4\,(2\cos^6\theta + 15\cos^4\theta\sin^2\theta + 3\sin^6\theta)$
Extended Padé, 7-point	$\frac{1}{80}(\kappa L)^2$

these are fourth-order accurate, the explicit nine-point cross and the Padé five-point cross on the square mesh, and the Padé seven-point cluster on the triangular mesh. Not one of these is isotropic. A comparison of the θ-dependence of the two Padé schemes is shown in Fig. 8, one for the square mesh and one for the triangular. By using the triangular, rather than the square mesh, the ratio of the maximum to minimum error is reduced from 4 to 1.5, and the maximum error is reduced by a factor of about 2. Both the isotropy and the maximum error are significantly improved by the choice of triangular mesh.

Three of the schemes presented in the tables are isotropic in the lowest order truncation term, the explicit nine-point scheme on the square mesh, and both the explicit seven-point cluster and the extended Padé scheme on the triangular mesh. Of the two explicit methods, the seven-point cluster has less error than the nine-point square for fewer points. The two isotropic triangular schemes are compared in Fig. 9, where the superiority of the extended Padé scheme is clearly evident over a wide range of wave numbers. Also shown in the figure are the maximum and minimum values of the modified wave numbers produced by the simple explicit five-point cross on a square mesh. Its anisotropy and the superiority of the seven-point triangular cluster are obvious.

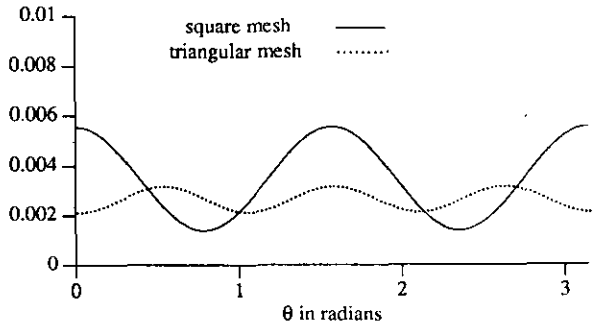

FIG. 8. Coefficient of the leading term of the phase speed error for the compact fourth-order schemes on the square and triangular meshes.

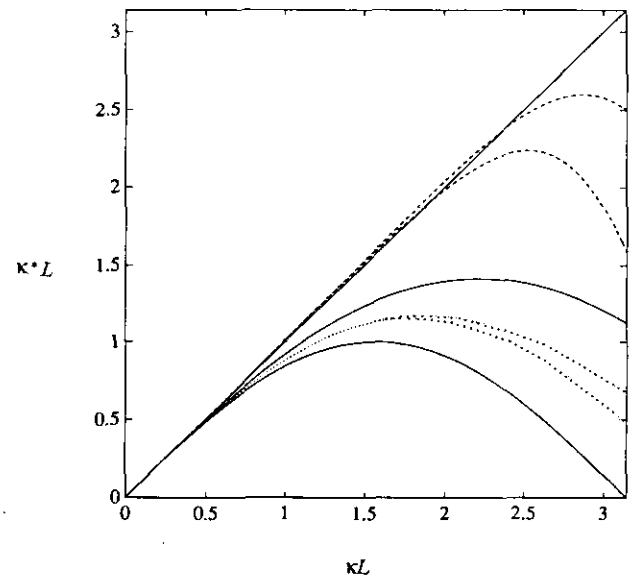

FIG. 9. Bounds of modified wave number for the explicit second-order five-point cross scheme on the square mesh (———), the second-order explicit scheme on the triangular mesh (···), and the extended wave number scheme on the triangular mesh (——).

6. CONCLUSIONS

The phase error and isotropy properties of various finite-difference schemes on grids consisting of regular triangles have been compared with similar schemes on square grids. The comparisons are based on a Fourier analysis of semi-discrete solutions to the two-dimensional linear convection equation. The finite-difference schemes presented on the triangular grid include a second-order method, a compact fourth-order method, and a modified compact method designed to extend the accurate wave number range of the numerical approximation. All of the schemes considered are centered and hence nondissipative. The results can be summarized as follows:

1. Based on the leading term of a Taylor series expansion of the phase speed error, the maximum error resulting from the explicit second-order scheme on the square grid is twice the minimum error while on the triangular mesh the error is isotropic.

2. For the fourth-order compact schemes, the ratio of the maximum to minimum error is 4 on the square grid and 1.5 for the triangular grid.

3. To lowest order, the extended-wave-number schemes have the same isotropy properties as the corresponding explicit second-order schemes.

In each case, the finite-difference scheme on the triangular grid reduces the anisotropy of the phase error in comparison with a similar scheme on the square grid.

REFERENCES

1. A. Bamberger, J. C. Guillot, and P. Joly, *SIAM J. Numer. Anal.* **25**, 753 (1988).
2. S. K. Lele, CTR Manuscript 107, Center for Turbulence Research, Stanford University, 1990 (unpublished).
3. R. Mullen and T. Belytschko, *Int. J. Numer. Methods Eng.* **18** (1982).
4. L. N. Trefethen, *SIAM Rev.* **24**, 113 (1982).
5. R. Vichnevetsky, *Int. J. Numer. Methods Fluids* **7**, 409 (1987).
6. R. Vichnevetsky and J. B. Bowles, *Fourier Analysis of Numerical Approximations of Hyperbolic Equations* (SIAM, Philadelphia, 1982).
7. R. Vichnevetsky and F. De Schutter, *Advances in Computer Methods for Partial Differential Equations*, edited by R. Vichnevetsky (AICA/IMACS, Rutgers University, NJ, 1975), p. 46.